SRI International

A LASER SCANNER FOR SOLDER JOINT IMAGING

Technical Note 302

August 1983

By: Alfred E. Brain, Senior Research Physicist
Robotics Department
Advanced Technology Division

Stephen T. Barnard, Senior Computer Scientist
Artificial Intelligence Center
Computer Science and Technology Division

SRI Project 3588

The research reported herein was supported
by the National Science Foundation under
Grant MEA-81144761.

SRI International®

333 Ravenswood Ave. • Menlo Park, CA 94025
(415) 859-6200 • TWX: 910-373-2046 • Telex: 334 486

ABSTRACT

This report gives a preliminary account of the construction of a low-cost laser system for providing data on defective solder joints on printed circuit boards. The system possesses high resolution, excellent signal-to-noise ratio, and a substantial depth of focus; the speed at which it produces data is limited only by the data rate of the computer input channel. Formulas are given from which design dimensions can be calculated for particular values of spot size and depth of focus (which translates into width of scanning track). Photographs are included of defective solder joints and scanned images. The practical limitations have to do with optical occlusion and consequent data loss.

FIGURES

1. Introduction

Automatic visual inspection of solder joints is a difficult problem, partly because there is no consensus as to what constitutes a defective joint, and partly because of the difficulty of obtaining images that clearly illustrate defects. Obviously, the most important property of a solder joint is that it provide a good electrical and mechanical connection between the component lead and the printed circuit board. A newly formed joint may temporarily provide a good electrical connection, but have a mechanical or structural defect that will cause it to fail after thermal cycling and vibration in the field.

There is wide disagreement about the effectiveness of visual inspection of solder joints. Some maintain that joints with so-called cosmetic defects, such as blow holes, drop outs, and cold solder, are statistically just as reliable as cosmetically acceptable joints, and that visual inspection is a waste of effort [1]. Others maintain that the surface quality of a joint is not important but that proper wetting and filleting are [2]. Regardless of these opinions, printed circuit board manufacturers continue to perform thorough and costly inspection of solder joints and to require rework of joints with such defects.

Paradoxically, automatic visual inspection of solder joints may be feasible for much the same reason that some maintain that visual inspection in general is unnecessary. The key point is that the detection of every cosmetic defect is probably not necessary (or feasible with an automatic system), but that a consistent monitoring of the appearance of joints (which is feasible) would be useful for maintaining process uniformity. In other words, it may not be necessary to detect and rework every blow hole; however, if many blow holes suddenly start appearing, something is likely to be wrong.

Two important properties of solder joints can be inferred from their visual appearance: the granularity of the material and the shape of the solder blob.

1.1. Detection of Cold Solder Joints

There is a long tradition to the effect that good solder joints have a shiny appearance, and that "dull-looking" joints (so-called cold solder joints) are likely to cause trouble later, even though electrical tests prove satisfactory. This may be because they are relatively brittle and therefore tend to crack after mechanical vibration and thermal cycling. Supposedly, dull-looking joints do not pass from liquid to solid by a smooth transition, but develop a large number of microcrystals that grow until they penetrate the meniscus; the gray appearance is caused by light scattered from the irregular surface. Figure 1 shows a number of rough solder pads immediately adjacent to a pad with a very smooth surface; it seem evident that the nucleation has been produced by contamination, rather than by local temperature variations. This board contains a substantial number of defects.

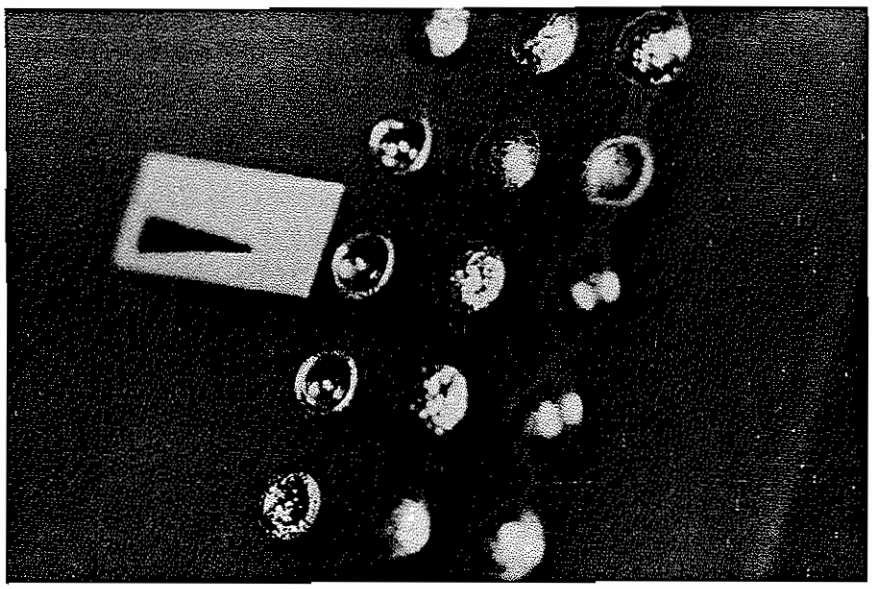

FIGURE 1 ROUGH SOLDER PADS ADJACENT TO PAD WITH SMOOTH SURFACE

Our premise was that a laser scanner would be able to distinguish between rough and shiny solder pads on the basis of the amount of scattered light. A shiny surface produces very little scatter, and therefore should appear to be black, whereas a rough surface produces a substantial amount of well-distributed diffuse scatter and should always be visible. Although this was found to be true with the equipment described herein, a number of additional requirements will need to be satisfied before a useful level of performance can be reached in an automatic inspection equipment, and some rather basic practical difficulties (e.g. obstructed vision) are to be expected.

1.2. Recognition of Solder-Joint Shape

The gross shape of a solder joint can indicate several important kinds of defects, among them improper wetting and filleting. One approach to detecting the shape of solder joints is to use structured light [3]. Another approach, which can be used with the image scans obtained with the laser scanner, is to estimate the shape from specular reflections. Assuming that the solder joint has a smooth surface (i.e. is not a cold joint), important information for its shape is contained in the pattern of specular reflection in the image (see Figure 1).

For example, if the joint exhibits so-called meniscus inversion, in which the joint is cup-shaped instead of normally rounded, the pattern of specular reflection will be a ring with possibly a spot near the center. The pattern for a normal joint will be simply a spot near the center.

2. A Simple Laser Scanner

Figure 2 shows a photograph of the laser scanner; the general optical and electrical layout is described by Figure 3.

The low-power HeNe laser has a power output of about 2 mW with a collimated beam-width of 0.65 mm. The beam is folded by two mirrors to provide a convenient layout, and then passed through a beam expander consisting of an infinity-corrected 16-mm microscope objective and a Schneider 105-mm f/4.5 Comparon enlarging lens. The enlarging lens is in a sliding mount and focuses an image of the pinhole stop in the beam expander onto the printed circuit board, where the lens-to-image distance is about 12 inches. The scanning mirror is mounted immediately after the enlarging lens and is driven by a General Scanning G-0612 galvanometer and AX-200 amplifier. The amplifier has variable gain and offset potentiometers that provide centering and sweep amplitude adjustments. The scanning waveform is produced by a Wavetek VCG-106 waveform generator, which also produces the square wave edge from which the timing pulses are derived. Since the A/D converter in the DEC LSI-11 computer is set up for an interval of 50 μs between samples, of which there are 512 per line, the minimum sweep time is about 26 ms. An equal sawtooth is used for the scan waveform (reducing the forces at the mirror, which is attached with cyanoacrylate cement), giving a recurrence rate of about 15 sweeps per second. The picture is stored in a 512 x 512 frame buffer (although the pictures shown are 256 x 256) with an 8-bit gray scale. The motion in the orthogonal direction is provided by a one-axis stage driven by a Slo-Syn stepper motor, where the step size is roughly 0.001 inch, the speed reduction being derived by good-quality gears having a ratio of about 8:1. The races on the slides use longitudinally recirculating balls, and the 0.001-inch translation steps are achieved with high precision. The available travel is 10 inches.

A Hamamatsu R888 9-stage side-window photomultiplier tube with S-10 photocathode is used to convert the light received by a small slit into an electrical signal. The dynamic range is very large (at least 10,000:1) and the maximum allowable signal from specular reflections is produced with only 500 V at the terminals of the phototube power supply. The maximum average signal, as read by a conventional moving-coil meter, should not exceed 100 μA, 500 μA peak. The total scanning time is about 30 seconds for a full 512 x 512 picture. Because the gamma (contrast) of a cathode ray tube is about 2.5 and its dynamic range is about 200:1, it is not possible to display all of the significant information without the use of a compression mechanism. We have used a logarithmic amplifier, where a 10:1 change in brightness is converted to a 1-V change in output signal. This guarantees that the brightness highlights do not overload the A/D converter, which does strange things if the input level exceeds 10 V. It is essential to shield out the stray room light, because the logarithmic amplifier enhances the response to weak signals (especially when fluorescent lighting is used, which has an appreciable 120-Hz modulation component).

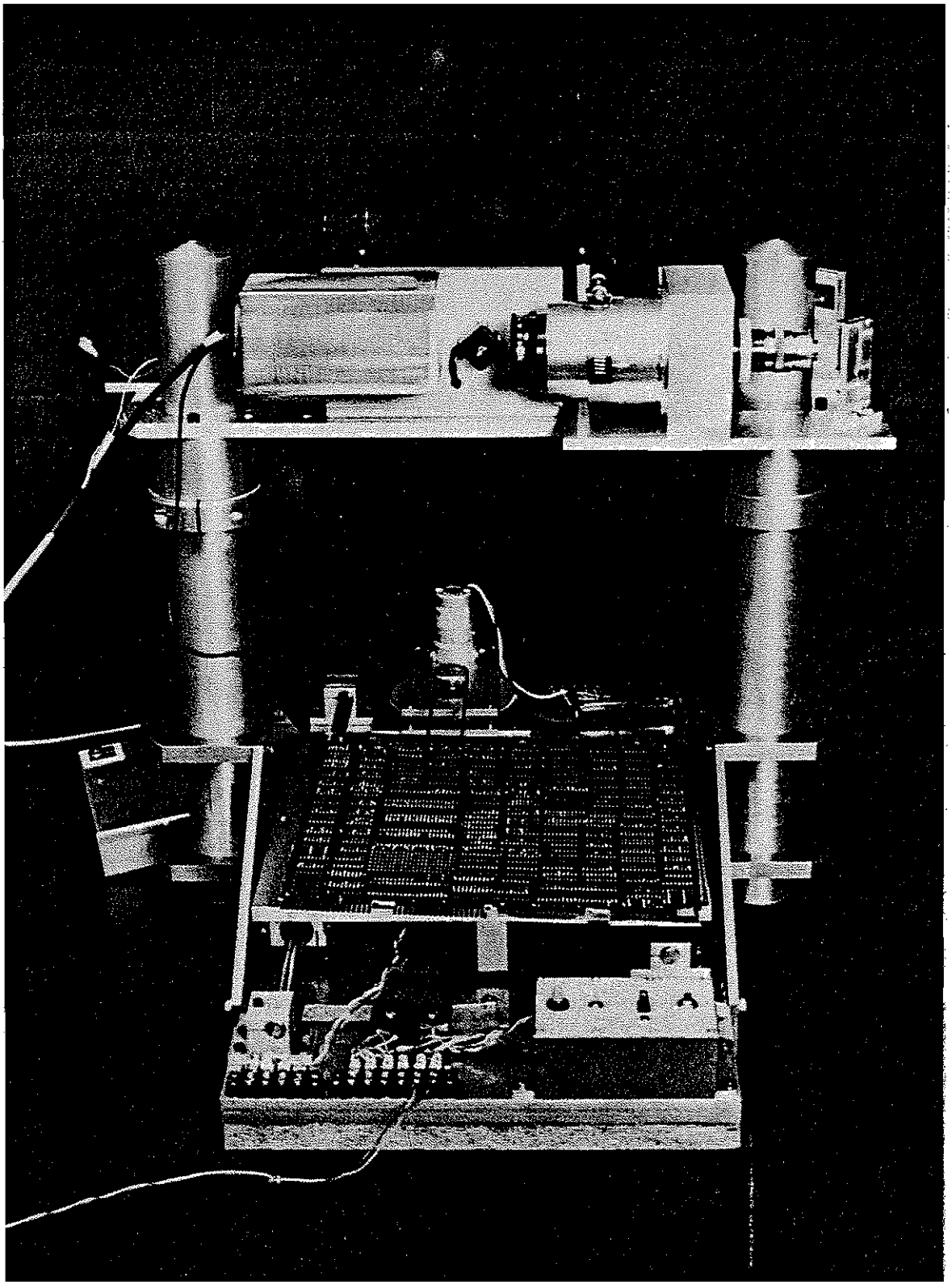

FIGURE 2 EXPERIMENTAL LASER SCANNER SYSTEM

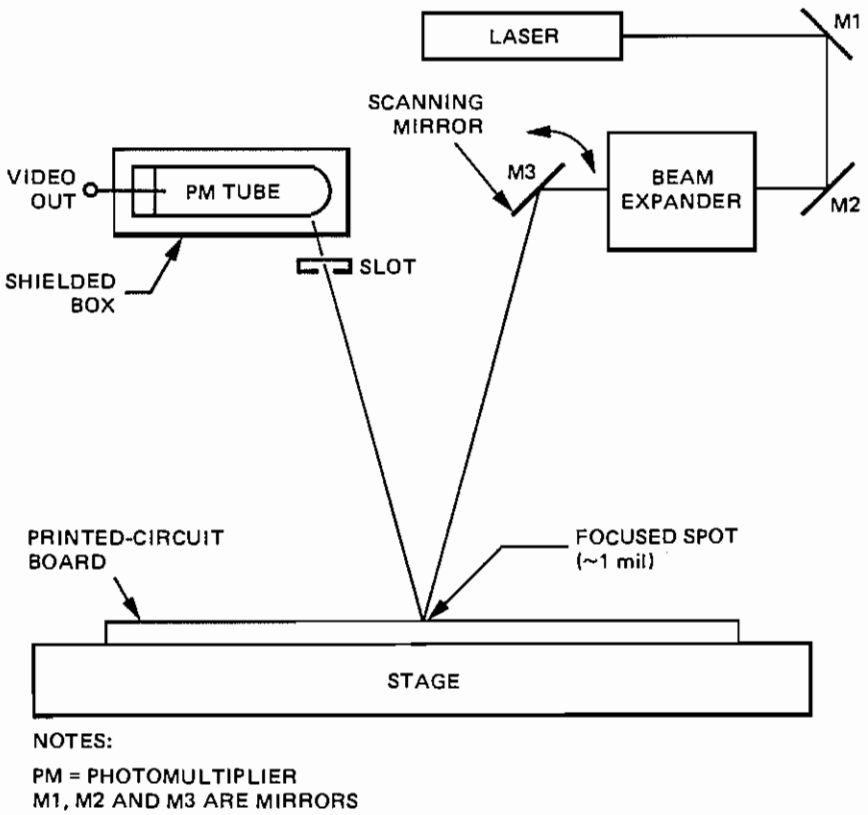

FIGURE 3 BLOCK DIAGRAM OF LASER SCANNING SYSTEM

The size of the slit in front of the photomultiplier is roughly 3 x 10 mm. If a very small slit is used, the photomultiplier becomes sensitive to laser speckle (which arises because the light is coherent); if the slit is too large the signal represents the integral over a large area with the consequent smoothing out of detail. The photomultiplier sensitivity is easily regulated by adjusting of the power supply voltage, which is stabilized to 0.005%. There is no problem with signal-to-noise ratio at this sampling rate, and the signal is virtually noise-free. Figure 4 shows the results from a readily available test object that is convenient for optimizing focus.

3. Spot Size and Depth of Focus

It is evident that we shall require the scanning spot to have a diameter much smaller than a trace width. We shall also require sufficient headroom between the scanning mirror and the board so that we do not lose too much light when the beam is at the limit deflection, and so that the spot does not go too far out of focus. Because we are dealing with an optical system that is not far removed from

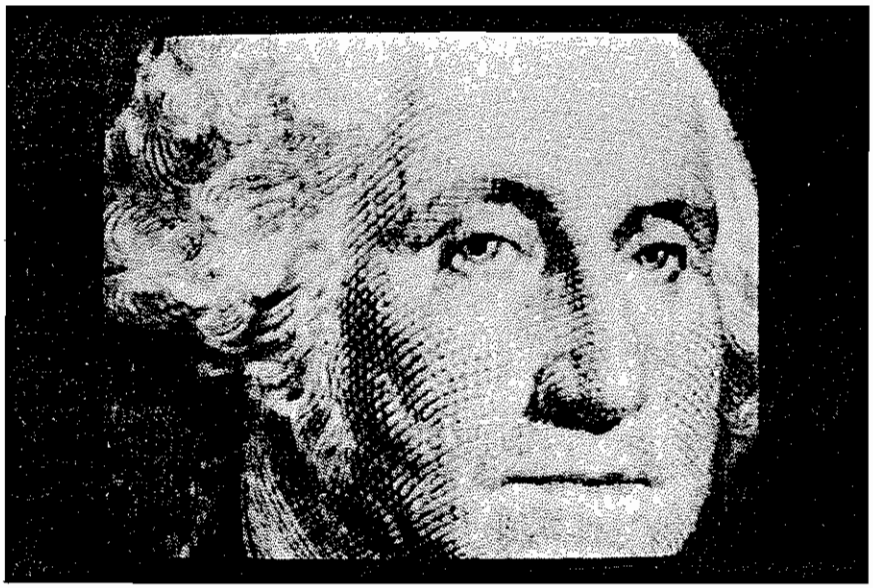

FIGURE 4 TEST OBJECT

being diffraction-limited, it is possible to provide good theoretical estimates for parameter values based on relatively simple analyses.

The standard diffraction theory of light [4] states that if we take a collimated beam of a given wavelength and pass it through a perfect positive lens (so that all of the components across the wavefront arrive at the focal point on the axis in phase), the diffraction pattern formed in a plane orthogonal to the axis at the focal point has an intensity distribution given by

$$I = \left[\frac{2J_1(z)}{z}\right]^2 ,$$

where $J_1(z)$ is a Bessel function of the first order.

The central bright spot is commonly known as the Airy disc, and its radius is

$$R = \frac{0.61\lambda}{n\sin(U)} ,$$

where λ is the wavelength of the light, n is the refractive index of the medium (i.e. $n = 1$), and U is the angle made by the extreme ray with the axis. For HeNe lasers, $\lambda = 632.8$ nm; if $U = 0.01$ the radius of the Airy disc is 0.039 mm, i.e. the spot diameter is about 0.003 inch. This is a good starting place for our application. We shall of course see detail smaller than the spot size by a factor of two or three, depending on the contrast.

The above calculation defines the semiangle of the light coming to a focus at the board, and thus it specifies the size of the deflecting mirror at the galvanometer when we choose the clearance between the mirror and the board. Let us assume a clearance of 10 inches. Since $U = 0.01$, then the beam width at the mirror is 0.2 inch, and a convenient mirror size would be 0.3 x 0.5 inches; the mirror is given a rectangular or elliptical shape, since it is mounted obliquely and is being deflected to provide the scan. A mirror of this size has appreciable inertia and exerts a significant influence on the galvanometer; that is, the voltage across the galvanometer does not define its position under dynamic conditions. For applications in which it is necessary to read the position of the mirror, it is possible to obtain galvanometers fitted with auxiliary coils that provide position readout.

In determining the size of the scanning mirror, we have also defined the size of the beam-expanding telescope between the laser and the mirror. If the width of the cone is 0.2 inch at the mirror, the telescope must be slightly larger at the adjacent lens, say 6 mm. This must be derived from the 0.65-mm beam at the laser output window; thus a beam expander of the order 9:1 would be appropriate.

To estimate the depth of focus, h, we can assume a geometrical spot diameter equal to the diffraction spot size calculated above (Figure 5):

$$h = \frac{2R}{\tan(U)}$$

If $2R = 0.003$ inch, and $U = 0.01$, then $h = 0.3$ inch. If the semiwidth of the scanning track on the board is W, then $W^2 = 2(0.3\text{inch})20 = 12$, and $W = 3.5$ inches. Thus, depth-of-focus considerations will allow the use of a scanning track 7 inches wide; in practice, the fall-off in illumination may require this to be reduced somewhat. However, the fall-off is mitigated to some extent by the use of a logarithmic amplifier in series with the photomultiplier output. Lost detail in the blacks can often be recovered by cutting down on the stray or secondary-scatter light, which reduces the modulation level when a logarithmic amplifier is used. The photomultiplier does not run out of dynamic range (saturate) for peak currents less than 300 μA, and its working range is in excess of 100,000:1 for tubes with standard levels of dark current. Even greater ratios are possible for selected tubes, although in this application they are unlikely to confer any practical benefit. The logarithmic amplifier renders the gain adjustment much less sensitive; in its absence setting up is somewhat critical.

4. Results

The behavior of the laser scanner shown in Figure 3 agrees well with the above theory in regard to both resolution and depth of focus. Because the beam expander was constructed from available materials, its performance is somewhat less than

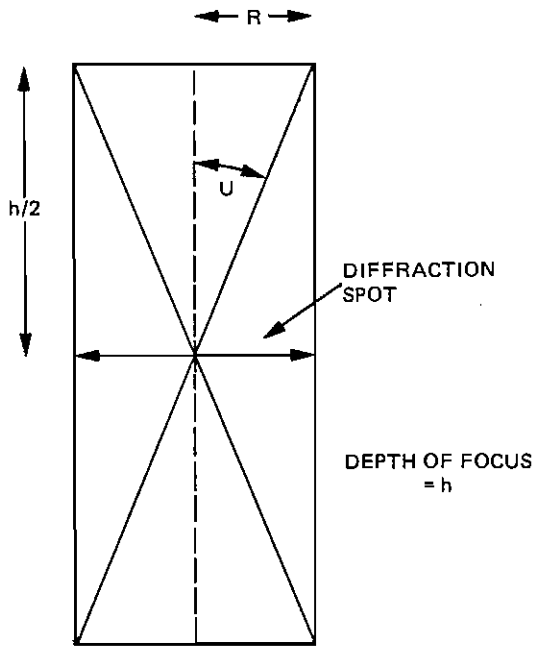

FIGURE 5 CALCULATION OF DEPTH OF FOCUS

optimum and its expansion ratio is on the low side. Accordingly, the angle subtended by the light is marginally low, and the depth of focus marginally high. Although the power level in the scanning beam is only 1 mW, the photomultiplier gives its maximum allowable output current with the power supply set to 500 V, conservatively, thus demonstrating that there is ample light for an excellent signal-to-noise ratio. The lines on the Starrett scale in Figure 6 are 0.010 inch apart.

Figure 6 also shows two of the practical problems. There is a small amount of line-to-line jitter in the image as shown by the 0.010 inch marks on the scale, but it is much less than one sees in the traces on the printed circuit board behind it. This apparent jitter is caused by the changes in surface curvature of the underlying board. The solder bridge tying two traces in the top right part of the picture has extreme curvature in the middle of the link; because it has a shiny surface, very little light is scattered into the photomultiplier.

It seems clear that this type of scanner could be used to inspect traces on bare boards — it is capable of generating an analog signal with a bandwidth of 100 MHz with excellent signal-to-noise ratio. A low-dark-current photomultiplier adds virtually no noise to the signal, and behaves as a pure photon counter. The signal-to-noise ratio varies as the square root of the number of photoelectrons (N) leaving the photocathode in the sampling interval; if N is too small, it may be increased by raising the laser power.

The principal difficulties with this equipment are associated with geometry, rather

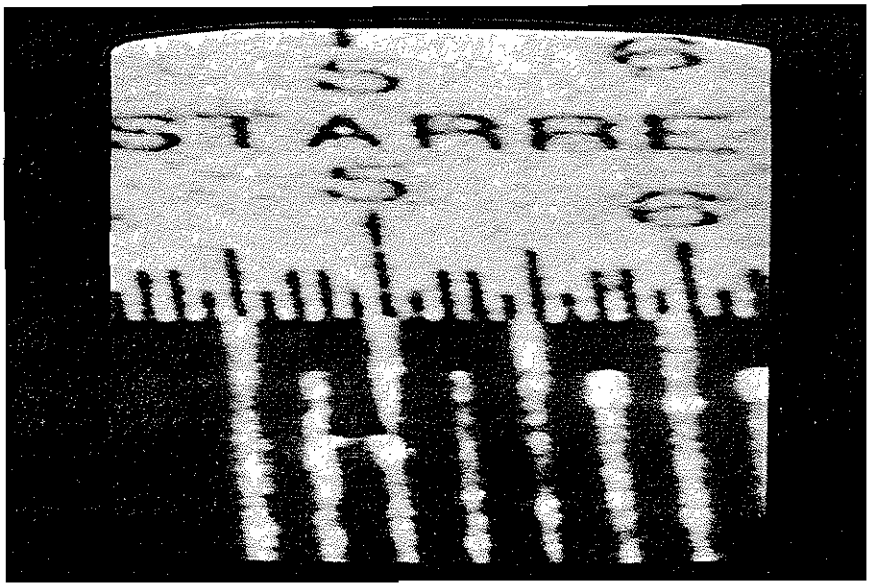

FIGURE 6 IMAGE FROM STARRETT SCALE

than with the device itself. It is essential that the light scattered from the laser spot not be obstructed on its way to the photomultipler; otherwise, there is no signal. So long as we are dealing with solder surfaces that do do not make an angle in excess of 20 degrees to the horizontal everything is straightforward; however, when the meniscus drops down inside an eyelet (as in Figure 1), the only light receivable may be tertiary scatter. Equally, there may be very little signal accessible from a tag carrying a massive globule (Figure 7). A related problem is the solder ball (Figure 8). When this is scanned (Figure 9) at normal incidence, it shows a large area bright central spot, which is rare, but could be confused with a with a large solder pad with a flat meniscus. The traces either side of the marker are heavily coated with varnish.

In a similar manner, blow holes (Figure 10) commonly occur very close to the leads, which may obstruct the view. Although it is quite possible to arrange for the scanning beam and the back-scattered beam to be collinear, this is generally undesirable, because the photomultiplier is then continuously blasted by specular returns. Blow holes that occur in the absence of component leads become reasonably visible (Figure 11).

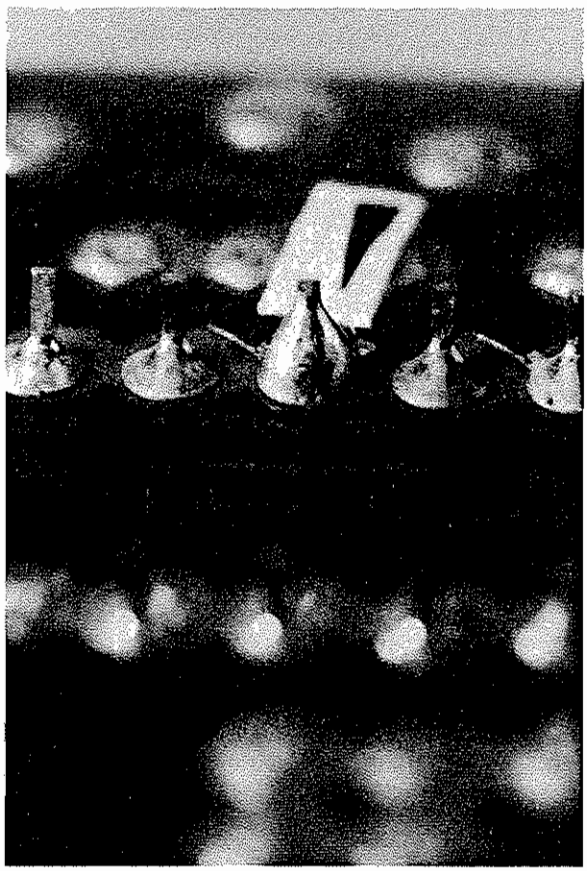

FIGURE 7 SOLDER GLOBULE

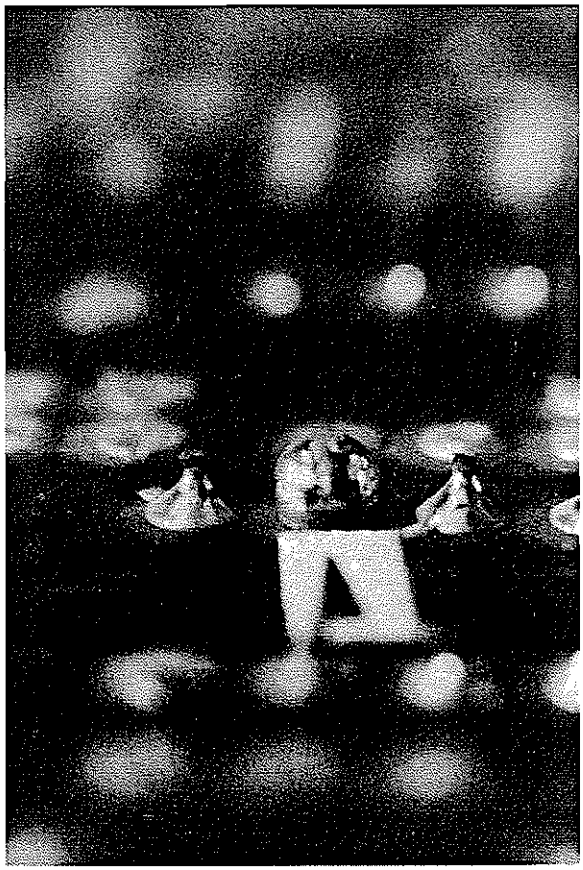

FIGURE 8 SOLDER BALL

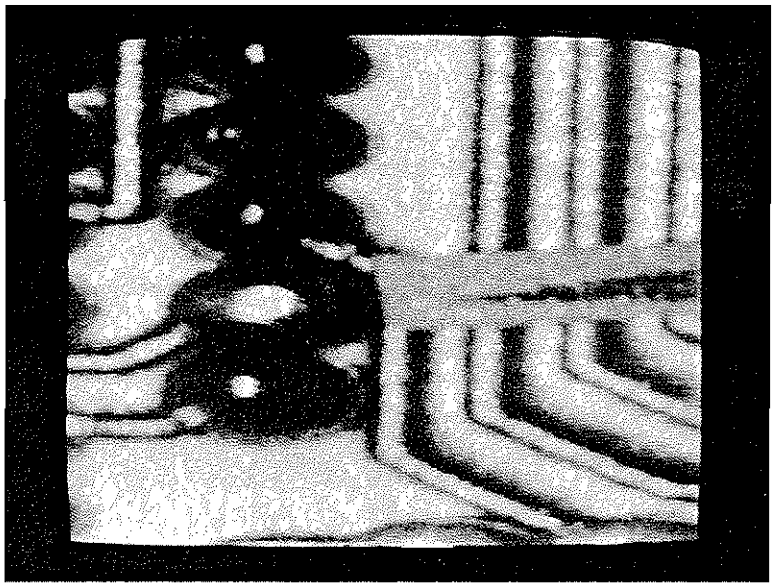

FIGURE 9 SCAN OF SOLDER BALL

In dealing with the component side of the board, the obstruction problem becomes even more difficult. Figure 12 shows a 45 degrees view of the pins of a chip, where one of the leads is incompletely wetted at the eyelet. This was marked as a defect, although to the unpracticed eye it is barely visible. The scanned image (Figure 13) shows a substantial specular reflection at each solder meniscus, with appreciably less response for the marked joint. However, the board had to be held at 45 degrees to avoid interference in the optical path.

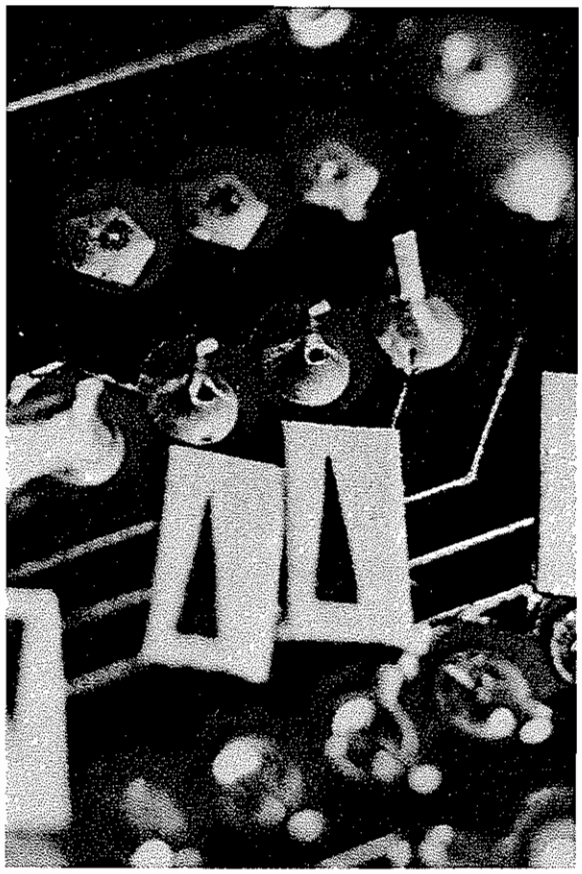

FIGURE 10 BLOW HOLES

FIGURE 11 SCAN OF BLOW HOLE

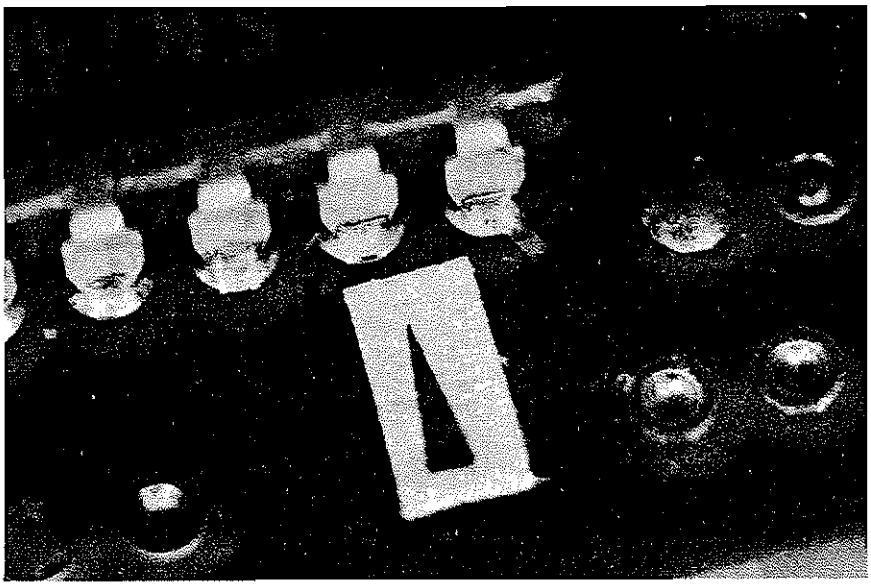

FIGURE 12 DEFECTIVE CHIP CONNECTION

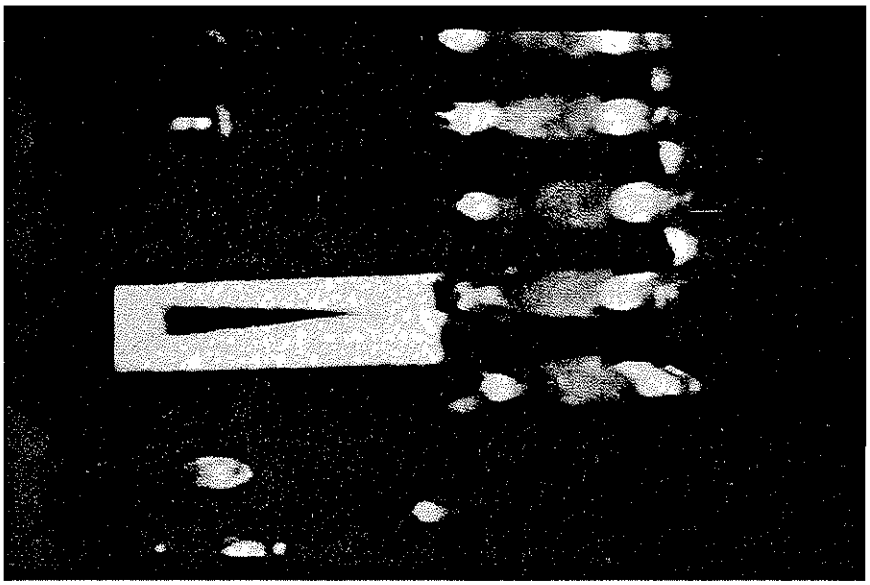

FIGURE 13 SCAN OF DEFECTIVE CHIP CONNECTION

5. Conclusions

The low-power laser scanner that has been described exhibits high resolution, a substantial depth of focus, very high signal-to-noise ratio combined with wide dynamic signal range. It is low in cost, and stable in operation.

The observed deficiencies have primarily to do with the geometry of the environment, so that the photomultiplier cannot see the scanning spot. This problem can be circumvented by the use of several receivers rather than just one.

ACKNOWLEDGMENT

The research reported herein was supported by the National Science Foundation under Grant MEA-81144761.

We would like to thank the Institutet för Verkstadsteknisk Forskning (Institute for Production Engineering) in Göteburg, Sweden for supplying us with sample solder joints.

REFERENCES

1. Keller, J.D., "Can the U.S. Afford the Cosmetic Look in Soldered Joints?" Electrical/Electronic Assembly, pp. 38-41, (November 1973).
2. Woodward, J.P., "Does Appearance Indicate Solder Joint Circuits Manufacturing?", pp. 46-53 (January 1978).
3. Nakagawa, Y., "Automatic Visual Inspection of Solder Joints on Printed Circuit Boards," Proc. Society of Photo-Optical Instrumentation Engineers, Vol. 336, pp. 121-127 (1982).
4. R. S. Longhurst, Geometrical and Physical Optics, 3rd Edition, Page 244, Longman, London and New York, 1973.